Six-bit all-optical quantization using photonic crystal fiber with soliton self-frequency shift and pre-chirp spectral compression techniques*

Kang Zhe(康 哲), Yuan Jin-Hui(苑金辉)†, Li Sha(李 莎), Xie Song-Lin(解松霖), Yan Bin-Bin(颜玢玢), Sang Xin-Zhu(桑新柱), and Yu Chong-Xiu(余重秀)

State Key Laboratory of Information Photonics and Optical Communications, Beijing University of Posts and Telecommunications, Beijing 100876, *China*

(Received 28 January 2013; revised manuscript received 26 April 2013)

In this paper, we propose an optical quantization scheme for all-optical analog-to-digital conversion that facilitates photonics integration. A segment of 10-m photonic crystal fiber with a high nonlinear coefficient of 62.8 W^{-1}/km is utilized to realize large scale soliton self-frequency shift relevant to the power of the sampled optical signal. Furthermore, a 100-m dispersion-increasing fiber is used as the spectral compression module for further resolution enhancement. Simulation results show that 317-nm maximum wavelength shift is realized with 1550-nm initial wavelength and 6-bit quantization resolution is obtained with a subsequent spectral compression process.

Keywords: all-optical analog-to-digital conversion, photonic crystal fiber, soliton self-frequency shift, spectral compression

PACS: 42.65.Re, 42.65.Tg, 42.70.Mp, 42.81.Dp **DOI:** 10.1088/1674-1056/22/11/114211

1. Introduction

With the rapid development of ultra-wide-band applications such as high speed optical communications, advanced radar systems, real-time signal monitoring, and so on, the requirements for high performance analog-to-digital convertor (ADC) techniques have become more and more urgent.[1,2] The electrical ADC has been remarkably improved during the last decade, whose state of the art resolution and sample rate can reach 10-bit and several giga-samples per second respectively. However, it still can not meet the requirements of much higher sample rate systems due to its inherent electrical bottleneck of the sampling aperture and the comparator.[1–3] Fortunately, an all-optical ADC (AOADC) based on nonlinear optics effects can overcome the electrical field problems. Several effective schemes have been proposed for the quantization of the AOADC. For instance, Miao *et al.* and Oda *et al.* proposed 2-bit AOADC utilizing photonic crystals and supercontinuum spectrum slicing, respectively,[4,5] Ikeda *et al.* realized 3-bit resolution using a Sagnac interferometer,[6] Konishi *et al.* realized the state of art 5 and 6-bit resolution cascade operation of optical quantization and coding, with soliton self-frequency shift (SSFS) and spectral compression techniques.[7,8] However, in the scheme of the current highest 6-bit AOADC, a fiber module of more than 2-km was used for optical quantization, which is disadvantageous for photonics integration. In addition, no more than 100-nm frequency shift was obtained. This is a great limitation to the resolution enhancement.

In this paper, we present an AOADC utilizing 10-m photonic crystal fiber (PCF) instead of the 1-km high-nonlinear fibers in Refs. [7] and [8] as the SSFS module and 100-m dispersion-increasing fiber (DIF) as the spectral compression module, respectively. The frequency-shift effect and the spectral compression efficiency are simulated and discussed to verify the performance and the feasibility of our proposed approach.

2. Principle of operation

Highly efficient SSFS[9–12] and spectral compression based on DIF[13–16] are key techniques of this proposed approach. SSFS can be used to realize the optical quantization due to its temporal power dependence property of frequency shift, and spectral compression can further enhance the quantization resolution. Generally, we can analyze these nonlinear phenomena by solving the generalized nonlinear Schrödinger equation (GNLSE) which is represented as[17]

$$\frac{\partial A}{\partial z}+\frac{\alpha}{2}A+\frac{\mathrm{i}\beta_2}{2}\frac{\partial^2 A}{\partial T^2}-\frac{\beta_3}{6}\frac{\partial^3 A}{T^3}$$

*Project supported by the National Basic Research Program of China (Grant Nos. 2010CB327605 and 2010CB328304), the National High-Technology Research and Development Program of China (Grant No. 2013AA031501), the National Natural Science Foundation of China (Grant No. 61307109), the Research Foundation from Ministry of Education of China (Grant No. 109015), the Program for New Century Excellent Talents in University of Ministry of Education of China (Grant No. NECT-11-0596), the Beijing Nova Program, China (Grant No. 2011066), the Specialized Research Fund for the Doctoral Program of Higher Education of China (Grant No. 20120005120021), the Fundamental Research Funds for the Central Universities of Ministry of Education of China (Grant No. 2013RC1202), the China Postdoctoral Science Foundation (Grant No. 2012M511826), and the Postdoctoral Science Foundation of Guangdong Province, China (Grant No. 244331).

†Corresponding author. E-mail: yuanjinhui81@163.com

© 2013 Chinese Physical Society and IOP Publishing Ltd

$$= \mathrm{i}\gamma\left(|A|^2 A + \frac{i\lambda_0}{2\pi c}\frac{\partial}{\partial T}(|A|^2 A) - T_{\mathrm{R}} A\frac{\partial |A|^2}{\partial T}\right), \quad (1)$$

where α represents the attenuation, β_2 and β_3 are dispersion coefficients, γ is the nonlinear coefficient, and T_{R} is the Raman coefficient. SSFS is mainly effected by the last two terms (self-steepening and the Raman effect) in the right-hand side of Eq. (1), while spectral compression corresponds to the first SPM term on the right. By using the method of moment (MOM), the distinct physical meaning of frequency shift and the pulse width variation can be obtained. Extracting four parameters of pulse moment, we can obtain

$$\begin{aligned} E &= \int_{-\infty}^{\infty} |A|^2 \mathrm{d}t, \\ \sigma &= \frac{1}{E}\int_{-\infty}^{\infty} t\,|A|^2 \mathrm{d}t, \\ \Omega &= \frac{\mathrm{i}}{2E}\int_{-\infty}^{\infty}\left(A^*\frac{\partial A}{\partial t} - A\frac{\partial A^*}{\partial t}\right)\mathrm{d}t, \\ \rho^2 &= \frac{1}{E}\int_{-\infty}^{\infty}(t-\sigma)^2\,|A|^2\,\mathrm{d}t, \end{aligned} \quad (2)$$

where E is the energy moment, σ is the time-delay moment, Ω is the frequency shift moment, ρ is the root-mean square pulse-width moment, A is the complex amplitude of optical pulse. For the hyperbolic secant pulse, calculating derivative, substituting GNLSE, and making simplification, we can obtain the solution of this equation set as follows:

$$\begin{aligned} \frac{\mathrm{d}E}{\mathrm{d}z} &= -\alpha E, \\ \frac{\mathrm{d}\sigma}{\mathrm{d}z} &= \beta_2\Omega + \frac{\beta_3}{2}\Omega^2 + \frac{\beta_3}{6T^2}\left(1+\frac{\pi^2}{4}C^2\right) + \frac{\gamma E}{2\omega_0 T}, \\ \frac{\mathrm{d}\Omega}{\mathrm{d}z} &= -\frac{4T_{\mathrm{R}}\gamma E}{15T^3} + \frac{\gamma C E}{3\omega_0 T^3}, \\ \frac{\mathrm{d}T}{\mathrm{d}z} &= \frac{\beta_2 C}{T} + \frac{\beta_3}{T}C\Omega, \end{aligned} \quad (3)$$

where $T = \sqrt{12}\rho/\pi$ is the pulse width and C is the pulse chirp. In the base-order soliton case ($0.5 < N < 1.4$), $E = 2|\beta_2|/(\gamma T)$, and the frequency shift can be further simplified as

$$-\frac{32T_{\mathrm{R}}(\gamma P_0)^2}{15|\beta_2|}z < \Omega(z) < -\frac{4T_{\mathrm{R}}(\gamma P_0)^2}{15|\beta_2|}z. \quad (4)$$

It is evident that the frequency shift of SSFS is closely related to the parameters γ, P_0, and $|\beta_2|$. Much larger frequency shift values can be obtained by increasing γ and P_0 while decreasing $|\beta_2|$. In such a case, there is a tradeoff when designing a certain fiber.

From the last terms of Eq. (3), the increase of pulse-width T can be realized with a certain fiber-parameter configuration. For example, when the optical pulse transmits at the anomalous dispersion region ($\beta_2 < 0$) and $\beta_3 > 0$, $C < 0$, T will increase continuously with the increase of β_2, which means that the width of its spectrum can be correspondingly compressed. However, in most other cases, the variation of T can hardly be judged since there is a summation process of two opposite components. By utilizing a segment of DIF, such spectral compression can be easily obtained.

3. Simulation and discussion

According to the above theoretical analysis, we propose an optical quantization scheme utilizing PCF and DIF as the nonlinear processing medium. The schematic diagram is shown in Fig. 1. The initial analog signal is firstly sampled to a serial of optical pulses with different values of power. This result can be effectively realized by the optical parametric processing. In addition, for simulation only, an optical attenuator can be used to obtain the result of sampling. Then, the sampled discrete pulses are delivered into a segment of PCF. After the transmission in the PCF, different wavelength shifts according to different sampled powers can be obtained due to the SSFS effect, with which the optical quantization is realized. Quantized signals are subsequently delivered into the spectral compression module, which is a segment of DIF (by comparison, a 1.2-km complex structure consisting of several alternant combination of SMF and HNLF is utilized in Refs. [7] and [8]) and facilitates photonics integration due to its simple structure. At last, the final quantized signals are sent into an arrayed waveguide grating (AWG) to separate from each other.

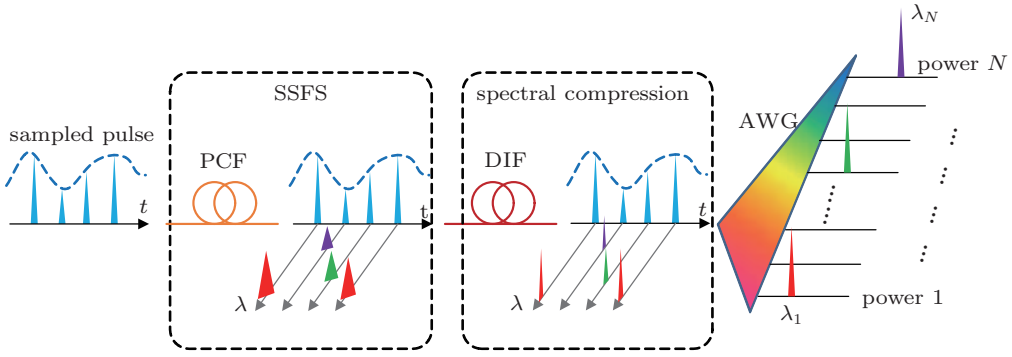


Fig. 1. (color online) Schematic diagram of proposed optical quantization. SSFS: soliton self-frequency shifting, PCF: photonics crystal fiber, DIF: dispersion increasing fiber, AWG: arrayed waveguide grating.

In our simulation, a hyperbolic secant optical source with 200-fs FWHM width, 40-GHz repetition, and 1550-nm center wavelength is utilized. For holding the base-order soliton, the peak power span is set from 220 W to 375 W. In the SSFS module, a 10-m PCF is utilized for optical quantization and its structure is shown in Fig. 2. The PCF has a core diameter of 1.7-μm and air ration of $d/\Lambda = 80\%$. The core is doped with 2% Ge. This structure results in a high nonlinear coefficient of 62.8 W^{-1}/km at 1550 nm. Other corresponding parameters at 1550 nm are calculated to be $\beta_2 = -152$ ps^2/km, $\beta_3 = -0.11$ ps^3/km, and $\alpha = 40$ dB/km, respectively.

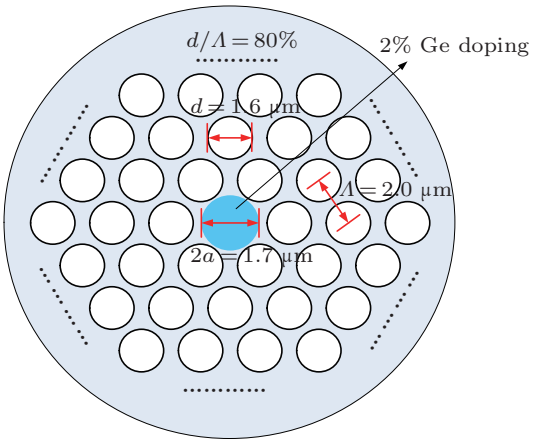


Fig. 2. (color online) Structural diagram of the high nonlinear PCF.

The frequency shift variation diagrams at several typical power points are shown in Fig. 3(a). With the increase in the initial peak power, the center wavelength of spectrum moves towards the longer wavelength region. At the maximum power of 375 W, the center wavelength is 1867 nm, which means 317-nm frequency shift is obtained. Figures 3(b) and 3(c) show the effects of different γ and β_2 on the frequency shift. All currents of the wavelength shift are proportional to the initial peak power. With the increase in γ, the increase of wavelength shift becomes square growth. By contrast, the wavelength shift is inversely proportional to $|\beta_2|$. However, it is not mean that larger frequency shift can be obtained by continually decreasing $|\beta_2|$. From the curve of $\beta_2 = -127$ ps^2/km, we can find that the wavelength shift starts to slow down and tends to be flattened after the peak power of 330 W. Therefore, the tradeoff among these parameters should be considered when designing appropriate fibers.

Resolution is a key measurement of optical quantization and can be represented as

$$N = \log_2\left(\frac{\lambda_{\text{shift}} + \Delta\lambda_{\text{FWHM}}}{\Delta\lambda_{\text{FWHM}}}\right), \tag{5}$$

where λ_{shift} is the wavelength shift after SSFS, $\Delta\lambda_{\text{FWHM}}$ is the FWHM of spectrum width. It is obvious that, to obtain a large resolution N, a larger λ_{shift} and a smaller $\Delta\lambda_{\text{FWHM}}$ should be achieved. Since we have obtained quite a large wavelength shift of 31-nm previously, a further decrease of $\Delta\lambda_{\text{FWHM}}$ will be much effective for the resolution enhancement. For realizing the spectral compression, a segment of 100-m DIF with parameters of $\gamma = 3.5$ W^{-1}/km, $\beta_2 = -0.6$ ps^2/km–-13.5 ps^2/km, $\beta_3 = 0.02$ ps^3/km, $\alpha = 0.4$ dB/km at 1550 nm is utilized. The DIF can be manufactured by properly increasing the core radius in its propagation direction, γ and β_3 are constant here because their variation along with the core size is typically negligible.[14,18] The spectrum diagram of non-chirp 200-fs (corresponding band-width is 12.7 nm) pulse propagating after the DIF is shown in Fig. 4(a). Different compression results corresponding to different initial peak power are calculated.

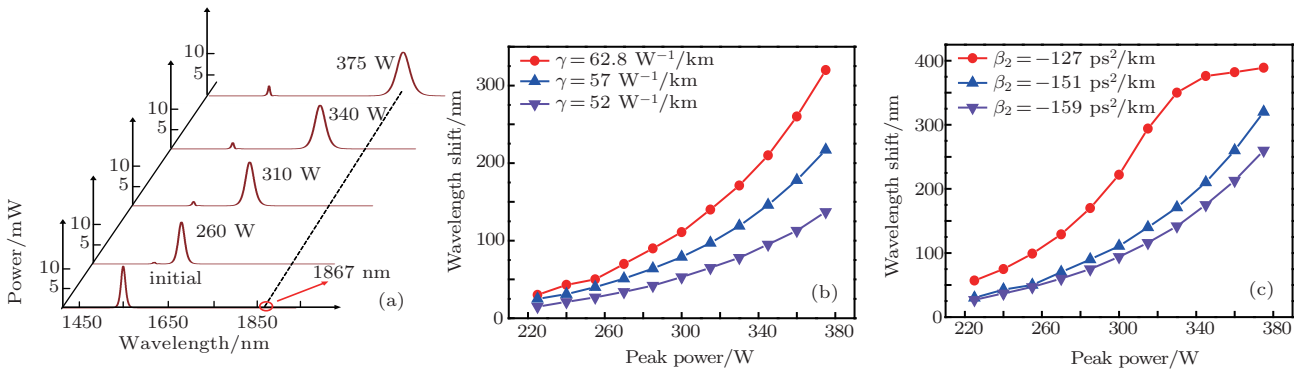


Fig. 3. (color online) Spectrum analysis after SSFS module. (a) Wavelength shift diagrams after SSFS with different peak power. (b) Peak power versus shift with different γ. (c) Peak power versus shift with different β_2.

The output spectrum widths decrease monotonically with the increase in the peak power. In addition, with the peak power of 80 W, a 4.5-nm FWHM can be obtained. This result means that the spectrum compression ratio (BW_in/BW_out) is 2.8. However, extra large wavelength shift occurs gradually with the increase in the peak power and 10-nm wavelength shift almost occurs with 80-W peak power. Such wavelength shift is harmful to the optical quantization because it will induce the spectrum overlapping of the neighbouring components. For further improvement, a pre-chirp process is added

before DIF transmission. This process can be realized by utilizing a small segment of single model fiber. Figure 4(b) shows the compressed spectrum with the initial chirp of −1. Comparing with the ones of $C = 0$, the compression ratio is enhanced while the wavelength shift is not extra large. Taking the one with peak power of 80 W for example, 4-nm spectrum width is obtained after DIF transmission. This means that the compression ratio is increased to 7.75. Combining with the 317-nm wavelength shift, we obtained previously, the 6-bit quantization resolution is obtained. Meanwhile, only 2-nm shift occurs and it is within the allowed scope because the final spectrum width is 4 nm. Figures 4(c) and 4(d) show the evolution diagrams of $C = 0$ and $C = -1$ with 80-W peak power, from which a more intuitional change occurs. Peak power versus compression ratio diagrams with different pre-chirps are shown in Fig. 5(a). Compression ratio monotonously increases with peak power in any case of chirp. However, more effective compression can be obtained when pre-chirp is −1. Figure 5(b) shows that the signal's bandwidth after DIF transmission increases monotonously with the decreases of pre-chirp and peak power. Since a smaller final bandwidth, which can be explained in Eq. (5), can directly enhance the quantization resolution, larger pre-chirp should not be chosen. Therefore, a pre-chirp close to −1 is the optimal setting.

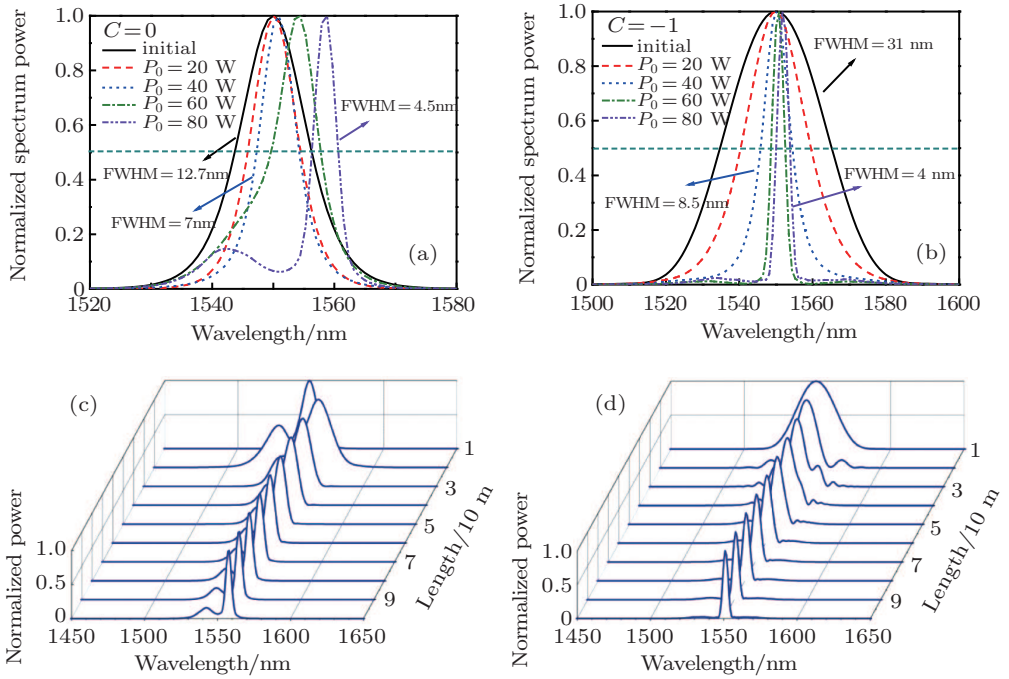


Fig. 4. (color online) Analysis of spectral compression. (a) Spectral variation with different P_0, $C = 0$. (b) Spectral variation with different P_0, $C = -1$. (c) Evolution diagram, $C = 0$, $P_0 = 80$ W, 200 fs. (d) Evolution diagram, $C = -1$, $P_0 = 80$ W, 200 fs.

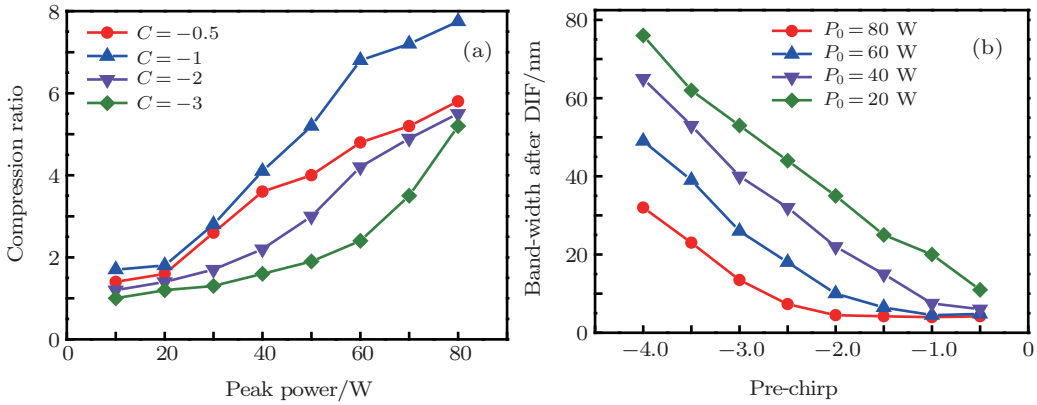


Fig. 5. (color online) Different peak powers and pre-chirp effects on compression ratio and final band-widths. (a) Peak powers versus compression ratio curve. (b) Pre-chirp versus final band-widths curve.

4. Conclusion

In summary, we proposed an optical quantization approach for all-optical analog-to-digital conversion utilizing SSFS and spectral compression techniques. By using PCF as the SSFS medium, 317-nm wavelength shift is obtained. To realize large scale wavelength shift, the necessary length of PCF is only 10 m. This means that the size of the SSFS module can be much smaller than those previously proposed based on

HNLF. With the effective spectral compression process using a short DIF of 100-m, we finally realize a 6-bit quantization resolution which is consistent with the state of art achievements. Negative pre-chirp close to -1 is proved to be efficient for increasing the spectral compression ratio and decrease the wavelength shift after the spectral compression process. Comparing with the pre-existing schemes, the total fiber length we used is only 110 m so that this proposed quantization scheme is more in line with the concept of miniaturization and integration. Therefore, our proposed quantization scheme for all-optical analog-to-digital conversion can meet the developing trend of optical signal processing devices and has great potential for future commercial applications.

References

[1] Khilo A, Spector S J and Grein M E 2012 *Opt. Express* **20** 4454
[2] Xu K, Niu J, Dai Y T, Sun X Q, Dai J, Wu J and Lin J T 2011 *Appl. Opt.* **50** 1995
[3] Valley G C 2007 *Opt. Express* **15** 1955
[4] Miao B L, Chen C H, Sharkway A, Shi S Y and Prather D W 2006 *Opt. Express* **14** 7966
[5] Oda S I and Maruta A 2005 *Photon. Technol. Lett.* **17** 465
[6] Ikeda K, Mohammad J, Namiki S and Kitayama K I 2005 *Opt. Express* **13** 4296
[7] Satoh T, Takahashi K, Matsui H, Itoh K and Konishi T 2012 *Photon. Technol. Lett.* **24** 830
[8] Konishi T, Takahashi K, Matsui H and Satoh T 2012 *International Conference on Transparent Optical Networks,* July 02, Coventry, UK, p. 1
[9] Shen X W, Yuan J H, Sang X Z, Yu C X, Rao L, Xia M, Han Y, Xia C M, Hou L T, Wu Z C and He X L 2013 *Chin. Phys. B* **22** 014102
[10] Yuan J H, Sang X Z, Yu C X, Xin X J, Li S G, Zhou G Y and Hou L T 2010 *Chin. Phys. B* **19** 074218
[11] Shen X W, Yuan J H, Sang X Z, Yu C X, Rao L, Xia M, Han Y, Xia C M and Hou L T 2012 *Chin. Phys. B* **21** 114102
[12] Fedotov A B, Voronin A A, Fedotov I V, Ivanov A A and Zheltikov A M 2009 *Opt. Lett.* **34** 662
[13] Liang R, Zhou X J, Zhang Z Y, Qin Z J, Li H P and Liu Y 2009 *Opt. Fiber Technol.* **15** 438
[14] Chuang H P and Huang C B 2011 *Opt. Lett.* **36** 2848
[15] Chuang H P and Huang C B 2011 *Photonics Conference,* October 9, Arlington, USA, pp. 569
[16] Nishizawa N, Takahashi K, Ozeki Y and Itoh K 2010 *Opt. Express* **18** 11700
[17] Agrawal G P 2007 *Nonlinear Fiber Optics* 4nd edn. (Salt Lake City: Academic Press) pp. 40
[18] Tamura K R and Nagazawa M 2001 *Opt. Lett.* **26** 762